



# Geostatistical analysis on the spatial variation of radiogenic elements in the crystalline basement of Grenville Province in the southwestern Québec

Hejuan Liu<sup>1,2</sup> · Patrick Were<sup>3</sup>

Received: 23 March 2018 / Accepted: 17 September 2018 / Published online: 30 October 2018  
© Springer-Verlag GmbH Germany, part of Springer Nature 2018

## Abstract

Accurate assessment of deep geothermal resources remains a challenge from the practical point of view. Parameter uncertainties and partial knowledge of initial conditions limit the prediction of subsurface temperatures using a variety of thermal models strongly unreliable, and the temperature is highly dependent on the radiogenic heat production in the geological layers mainly affected by a number of factors including the concentrations of uranium, thorium and potassium, and rock density. In this paper, geostatistical methods were applied to investigate the spatial distribution of radiogenic elements (e.g., uranium, thorium, potassium) and their corresponding concentrations and radiogenic heat production. A representative region measuring 35 km × 80 km in the southwestern Québec, and covering the domains of Portneuf-Mauricie, Morin Terrane and Parc des Laurentides in the Grenville Province was selected for this study because of its easy accessibility. Analysis results show that the concentrations of uranium, thorium and potassium for most rocks of the Grenville basement in the research region are in the range of 1–2 ppm, 3–10 ppm and 1–4%, respectively. Furthermore, 90% of the total samples analysed in this study show a uranium concentration of less than 3 ppm, 64% of the samples show a thorium concentration of less than 5 ppm, and 56% of the samples show a potassium concentration of less than 3%. This paper engaged both the ordinary kriging interpolation and sequential Gaussian simulation (SGS) methods to study the spatial distribution of radiogenic elements. Using density data for specific rocks, the distribution of radiogenic heat production in the study area of the southwestern Grenville Province was also simulated using the SGS method. Conclusively, results show that the difference between the minimum and the maximum value of radiogenic heat production is 30%, considering a significant proportion of heterogeneity in rock density.

**Keywords** Ordinary kriging · Sequential Gaussian simulation · Radiogenic elements · Crystalline basement

## Introduction

The extraction of deep geothermal energy has become a worldwide hot topic in recent years prompting innovative research in the reduction of drilling costs and development of deep reservoir stimulation technologies (Tester

et al. 2006). However, reliable assessment of geothermal resources at depth is very challenging because of the great uncertainties in the subsurface conditions (Fuchs and Balling 2016). Numerical simulations are quite a practical method to understand subsurface processes but require a solid theoretical background of physics and advanced computational capabilities (Vidal and Archer 2015). Taking the assessment of a specific deep geothermal reservoir, for example, in most cases, all numerical models of the subsurface fluid flow in a geothermal system will be strongly dependent on the knowledge about the geological structure, subsurface rock properties and so on. All these data are obtained from a multidisciplinary approach, including geology, geophysics, geochemistry, and drilling activities. The accuracy of a thermal model to estimate the spatial distribution of temperature at depth is directly related with the magnitude of the physio-chemical parameters (e.g., radiogenic elements

✉ Hejuan Liu  
hjliu@whrsm.ac.cn

<sup>1</sup> State Key Laboratory of Geomechanics and Geotechnical Engineering, Institute of Rock and Soil Mechanics, Chinese Academy of Sciences, Wuhan 430071, China

<sup>2</sup> University of Chinese Academy of Sciences, Beijing, 100049, China

<sup>3</sup> Energie-Forschungszentrum Niedersachsen, Clausthal University of Technology (TUC), Am Stollen 19, 38640 Goslar, Germany

concentration, thermal conductivity etc.) and their spatial distributions (Li and Heap 2014).

Parameterization of the variables from local points to spatial distribution is the key to a reliable assessment of geothermal resources. There are many methods for spatial interpolation of variables (such as radiogenic elements concentration and thermal conductivity) related with geothermal energy assessment which may be classified into three categories (Li and Heap 2008): (1) geostatistical; (2) non-geostatistical; and (3) a combination of both. Geostatistics can be regarded as a collection of numerical techniques that deal with the characterization of spatial attributes, primarily employing random models based on limited sample data points (Olea 1999). In geostatistics, semi-variogram analysis, kriging interpolation and stochastic simulation are often involved. Variogram-based models, also called the two-point statistical models, are widely applied in the simulation of groundwater flow, environmental pollution, distribution of mineral resources and geothermal resources (Yamamoto 2000; Yang et al. 2008). Among them, the kriging interpolation method is widely applied to estimate the mean value of a variable at un-sampled locations by calculating the weights of observation samples at un-sampled locations in a local region (Nshagali et al. 2015). Among the large series of kriging interpolation methods, ordinary kriging (OK) can provide an optimal unbiased estimation in a local region.

Another variogram-based model, stochastic simulation is a general means for generating multiple realizations of a specific variable, rather than a map of local best estimates produced by kriging (Goovaerts 1997a, b; Song et al. 2013). Unlike kriging, stochastic simulation approach takes into account both the spatial variation of original data at sampled locations and the variation of estimates at un-sampled locations (Delbari et al. 2009). The most widely used stochastic simulation method, Sequential Gaussian simulation (SGS), is based on the Monte Carlo method and overcomes the smoothing effect induced by the kriging interpolation method, is often applied in the description of the distribution of continuous variables (such as porosity, permeability, concentration of elements etc.), in the field of hydrogeology, ecology, pedology, mining, petroleum etc. (Dubrule 1989; Caers 2005; Doyen 2007). In comparison with the partial optimization of the estimator value in the kriging interpolation algorithm, geostatistical stochastic simulation is able to assess the spatial distribution of any desired variables while analysing its uncertainty (Soltani et al. 2013) and realizing the optimization of the estimator values in the whole region through multiple realizations based on the same input data (Zhao et al. 2010).

In addition to the high temperature hydrothermal system that are mainly related with the magmatic system, in the exploration for the production of deep geothermal energy potential sites are often located in the hot dry rocks, which are reservoirs with high concentrations of radiogenic elements, including uranium, thorium and potassium. A good

example of this is the high-quality geothermal resource located in the Cooper Basin of Australia. Due to the presence of high heat generating granites in the range of 3.8–8.7  $\mu\text{W}/\text{m}^3$ , high temperature geothermal resources are attained (Meixner et al. 2012). Parameters involved in the calculation of radiogenic heat production include the concentration of uranium, thorium, potassium and rock density. However, because of the limited number of samples retrieved from the subsurface and the strong heterogeneity of the lithology associated with the geological formations, it is difficult to have a clear understanding on the spatial distribution of radiogenic heat produced over a large region.

The assessment of the geothermal potential in the western St. Lawrence Lowlands Basin located in the southwestern Québec requires a clear understanding of the characteristics of its crystalline basement, especially its radiogenic properties. However, because of the limited number of samples and the partial knowledge of the uncertainties associated with the prediction of the distribution of radiogenic elements in the western St. Lawrence Lowlands Basin, it is logic to investigate the radiogenic characteristics in the outcrops from the neighboring regions (e.g., Portneuf-Mauricie domain, Parc des Laurentides domain, Morin Terrane, etc.).

The main objective of this paper is to understand the radiogenic characteristics of the Grenvillian basement located in the northern part of the western St. Lawrence Lowlands Basin using geostatistical methods. Both the ordinary kriging (OK) and sequential Gaussian simulation (SGS) methods were applied to investigate the spatial distribution of the radiogenic elements to get their optimizations in the local and whole region, respectively. The spatial distribution of the radiogenic heat production is also studied statistically using the SGS to obtain optimal results at the regional scale.

## Study area

The study area lies in the Grenville Province (Fig. 1a), whose geology is composed of high-grade metamorphic terranes and stacks of thrust sheets along ductile shear zones (McLelland et al. 2010), equivalent to the roots of a Himalayan-type collisional orogeny (Rivers 1983, 2015; Davidson 1984; Dufréchoy et al. 2014). The north–south strike of the Grenville structural belt extends from Canada southward into the subsurface of the Appalachian Foreland Basin (Shumaker and Wilson 1996), which belongs to part of the Appalachian orogeny that extends from Newfoundland to North Carolina (Fichter and Richard 1993; Hatcher et al. 2004). Rocks of Grenvillian age outcrop in the southwestern Québec in the lithotectonic domains of Morin Terrane, Portneuf-Mauricie and Parc des Laurentides.

St. Lawrence Lowlands Basin, located in southwestern Québec, is comprised of Cambrian–Ordovician sedimentary

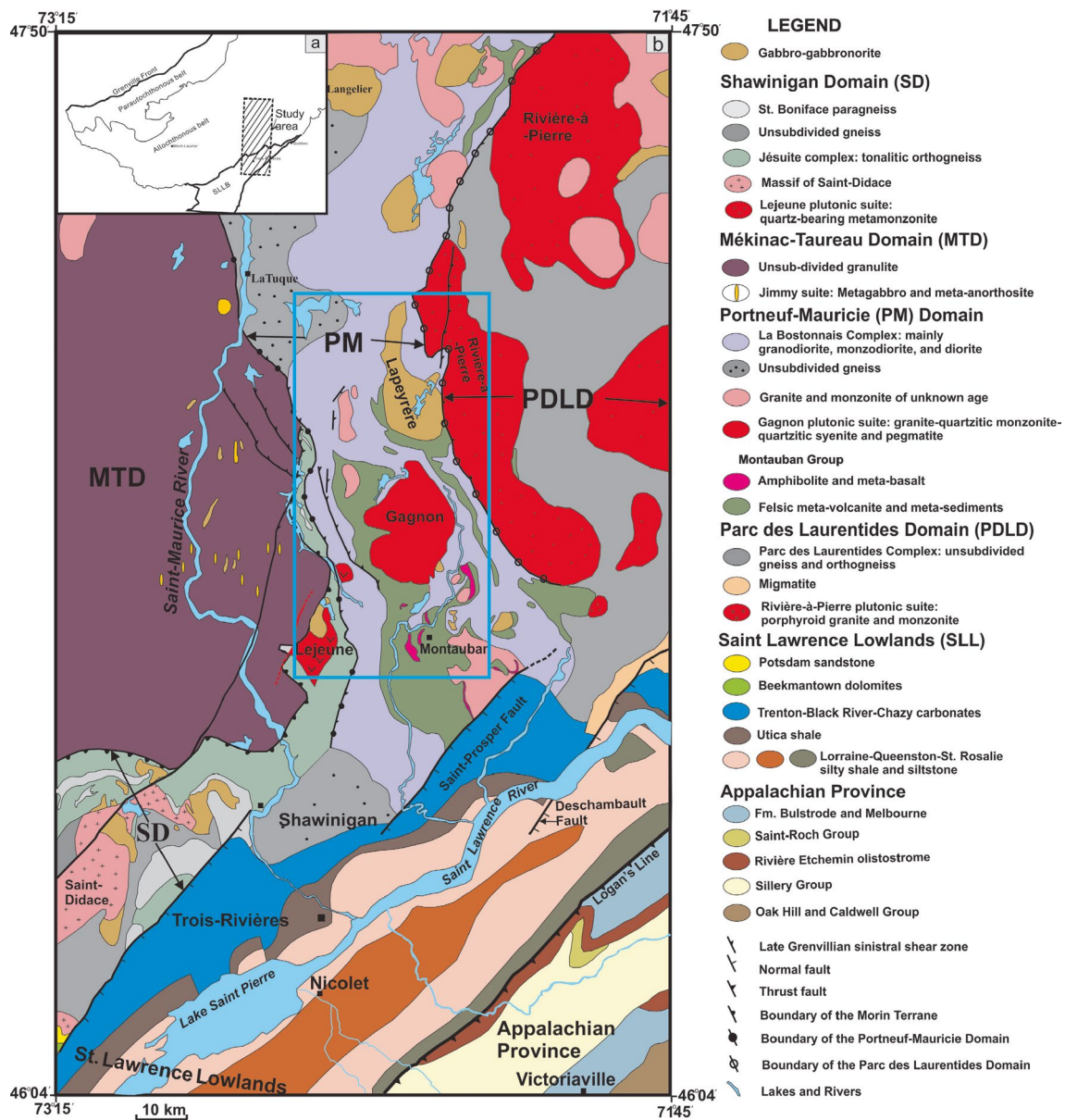


**Fig. 1** **a** Location map of the southwestern Grenville Province and St. Lawrence Lowlands Basin (SLLB) in Québec Province. **b** Detailed geological map of the study area (composed of Grenville aged rocks) in the southwestern St. Lawrence Lowlands Basin and its neighbor-

ing regions including Portneuf-Mauricie (PM) domain, Shawinigan domain (SD) that is part of the Morin Terrane (MT) and Parc des Laurentides domain (PDL) (modified from Nadeau and Brouillette 1994, 1995; Sappin 2012)

rocks and a crystalline Grenvillian basement composed of rocks including granite, granitic gneiss, paragneiss, orthogneiss, gabbronorite, monzonite, and amphibolite (Tremblay et al. 2003; Lavoie et al. 2009; Pinti et al. 2011). Figure 1b shows simplified detailed geological map of the western part of the St. Lawrence Lowlands Basin and its neighboring regions in the Grenvillian province including the Portneuf-Mauricie (PM) domain, Morin Terrane (MT) and Parc des Laurentides domain (PDL). The area bounded by the blue rectangle and covering the intrusions of Gagnon, Lapeyriere and Montauban group was selected in this paper. Figure 2 shows the sampling

locations and concentrations of uranium, thorium and potassium in the study area.

## Methodology

### Sampling and analysis methods

170 samples collected using RS-230 spectrometer together with data obtained from the Quebec Ministère des Ressources naturelles et de la Faune (SIGEOM database 2018)

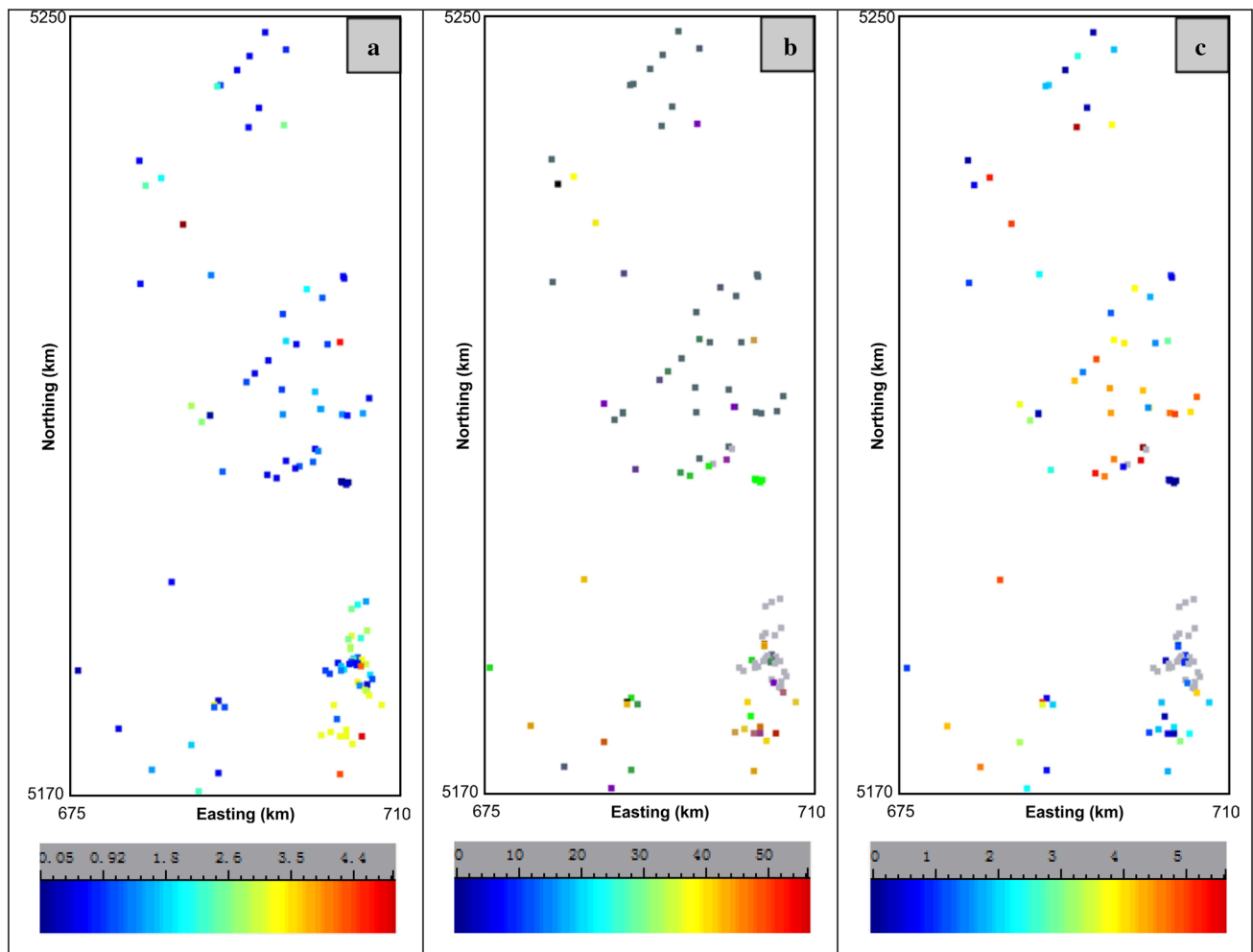


**Fig. 2** Sampling locations and concentration of **a** uranium (ppm), **b** thorium (ppm) and **c** potassium (%) in the study area of the Grenville Province

are prepared for the input data. From the SIGEOM database, samples for uranium concentration were analysed based on NAA-neutron activation method and samples for thorium concentration were analysed based on NAA and X-ray fluorescence, while those for potassium concentration were analysed based on X-ray fluorescence and plasma emission spectrometry. When a much larger region with longitudes ranging from  $73^{\circ}15'$  to  $71^{\circ}45'$  west of Greenwich and latitudes ranging from  $46^{\circ}04'$  to  $47^{\circ}50'$ , see Fig. 1b, in the Grenville Province (covering Morin Terrane, Portneuf-Mauricie domain, Parc des Laurentides domain) is considered, a total number of 404 uranium, 357 thorium and 411 potassium samples were collected.

### Ordinary kriging estimation method

Ordinary kriging estimation method on this paper aims to predict the value of a variable (e.g., concentration of radiogenic elements, rock density, thermal conductivity etc.) over

any un-sampled location based on the values of the scattered measured data points available (Vidal and Archer 2015). As a popular tool of interpolation and extrapolation, kriging is a generic name adopted by geostatisticians for the family of generalized least-squares regression algorithms, which was developed by Matheron (1963) based on the pioneering work of Krige (1951).

The basic form of the kriging estimator can be written as (Goovaerts 1997a, b)

$$Z^*(x_0) - m(x_0) = \sum_{i=1}^n \lambda_i [Z(x_i) - m(x_i)], \quad (1)$$

where  $x_0$  and  $x_i$  are location vectors at the estimation point and one of the neighboring data point, indexed  $i$ ;  $n$  is the number of data points in local neighborhood used for estimation of  $Z^*(x_0)$ ;  $m(x_0)$ ,  $m(x_i)$  are the expected means of  $Z(x_0)$  and  $Z(x_i)$ , respectively;  $\lambda_i$  is the kriging weight assigned to

datum  $Z(x_i)$  at the estimation location point  $x_0$ ; note that the same datum may produce different weights at different estimation locations.

The number of data points involved in the estimation as well as their weights may change from one location to another. However, ordinary kriging (OK) allows one to account for the local variation of the mean by limiting the domain of stationarity of the mean to the local neighborhood centered at the location point  $x_0$  (Goovaerts 1997a, b).

The following generic equation can be used to describe the linear regression ordinary kriging estimator at a specific location:

$$Z_{OK}^*(x_0) = \sum_{i=1}^n \lambda_i^{OK} Z(x_i), \tag{2}$$

where  $Z_{OK}^*(x_0)$  is the ordinary kriging estimator at the location  $x_0$ ;  $x_1, \dots, x_n$  is a series of observation locations and  $Z(x_1), \dots, Z(x_n)$  are the corresponding measurement values at the observation or sampling locations;  $\lambda_i^{OK}$  is the vector of ordinary kriging weights for the surrounding data points and satisfy the relationship as follows:

$$\sum_{i=1}^n \lambda_i^{OK}(x_0) = 1. \tag{3}$$

Based on the unbiased condition and the relation that

$$C(h) = C(0) - \gamma(h), \tag{4}$$

where  $C(0)$  is the sill value in the semi-variogram diagram  $\gamma(h)$ .

The ordinary kriging system is expressed in terms of covariant (semi-variograms) as

$$\begin{cases} \sum_{i=1}^n C(x_i - x_j) \lambda_i^{OK}(x_0) + \mu = C(x_0 - x_j), & (j = 1, \dots, n) \\ \sum_{i=1}^n \lambda_i^{OK}(x_0) = 1, \end{cases} \tag{5}$$

where  $\mu$  is the Lagrangian parameter.

The ordinary kriging system can be written in the matrix form as

$$K_{OK} \lambda_{OK}(x_0) = M_{OK}, \tag{7}$$

and the ordinary kriging weights can be described as  $[\lambda_{OK}] = [K_{OK}]^{-1} [M_{OK}]$ :

$$\begin{bmatrix} \lambda_1 \\ \lambda_2 \\ \dots \\ \lambda_n \\ -\mu \end{bmatrix} = \begin{bmatrix} C_{11} & C_{12} & \dots & C_{1n} & 1 \\ C_{21} & C_{22} & \dots & C_{2n} & 1 \\ \dots & \dots & \dots & \dots & \dots \\ C_{n1} & C_{n2} & \dots & C_{nn} & 1 \\ 1 & 1 & 1 & 1 & 0 \end{bmatrix}^{-1} \begin{bmatrix} C_{01} \\ C_{02} \\ \dots \\ C_{0n} \\ 1 \end{bmatrix}. \tag{8}$$

The solution of  $\lambda_i$  depends on the solution of the covariance  $C_{ij}$  between the point locations  $i, j$ . This requires the selection of a reasonable semi-variogram theoretical model (e.g., spherical, exponential, Gaussian model etc.) to fit the experimental data.

### Sequential Gaussian simulation method

The sequential Gaussian simulation (SGS) requires a standard Gaussian data with mean of 0 and variance of 1. Therefore, the input data should be transformed into a normal (Gaussian) distribution through a quantile transform. In the SGS algorithm the mean and variance of the Gaussian distribution at any location point along the simulation path is estimated by the kriging estimate and the kriging variance (Vidal and Archer 2015). Rather than choosing the mean as the estimate at each grid node like in the kriging interpolation method, SGS uses a random deviate from the normal distribution. This random deviate is selected according to a uniform random number representing the probability level. The variable at each unknown grid node is simulated sequentially according to its normal conditional cumulative distribution function (ccdf). During multiple realizations, it uses not only the original data but also all the previously simulated values.

The detailed workflow of the conditional simulation of a continuous variable  $Z(x_i)$  in a Gaussian space during one realization have already been investigated by many previous authors (e.g., Deutsch and Journel 1998; Remy et al. 2009; Soltani et al. 2013) thus not mentioned here. Randomization allows to perform multiple realizations including their mean values.

### Calculation of radiogenic heat production

When the concentration of a radiogenic element (e.g., uranium, thorium or potassium) is known, together with the values of rock density at the sampled locations, radiogenic heat production can be calculated using the following empirical function (Mareschal and Jaupart 2004; Rybach 1976, 1988):

$$A = \rho_r [9.52C_u + 2.56C_{Th} + 3.48C_k] \times 10^{-5}, \tag{9}$$

where  $\rho_r$  is the dry density of rock (in  $\text{kg/m}^3$ ),  $C_u$  is the uranium content (in ppm),  $C_{Th}$  is the thorium content (in ppm), and  $C_k$  is the potassium content (in %),  $A$  is the radiogenic heat production (measured in units of  $\mu\text{W/m}^3$ ).

## Results and discussion

### Concentration of radiogenic elements at sampled sites

In the study area (Fig. 1b), a region enclosed by longitudes in the range between  $73^{\circ}15'$  and  $71^{\circ}45'$  west of Greenwich and latitudes in the range between  $46^{\circ}04'$  and  $47^{\circ}50'$ , a total of 404 uranium data, 357 thorium data and 411 potassium data were collected. Comparing the concentration of radiogenic elements for different rock types, including granitic gneiss, paragneiss, quartzite, amphibolite, granite, diorite, quartz monzonite and gabbro-gabbro-norite that comprise the Precambrian Grenville Province (Fig. 3), it can be demonstrated that the distribution of radiogenic elements is very sparse in all types of rocks. In general, the concentration of uranium is in the range of 1–2 ppm for most samples (e.g., in granitic gneiss, amphibolite,

granite, diorite and quartz monzonite), although a little higher in quartzite and lowest in gabbro-gabbro-norite.

Similarly, the concentration of thorium for most rocks in the study area is in the range of 3–10 ppm, with gabbro-gabbro-norite and quartz monzonite having the lowest and highest values, respectively.

The concentration of potassium ranges from 1 to 4% in most rock types investigated, with granite and quartz monzonite showing the highest values.

According to the boxplot the average concentration of uranium, thorium and potassium is 1.78 ppm, 6.01 ppm and 2.64%, with a standard deviation error of 3.57, 7.27 and 1.85, respectively. It can also be observed that 90% of the total samples have uranium concentration of less than 3 ppm, 64% of the samples have thorium concentration of less than 5 ppm, and 56% of the samples have potassium concentration of less than 3%.

The cumulative distribution frequency diagrams (in Fig. 4), it can be seen that only 3 and 4% of the samples from the Portneuf-Mauricie domain and Morin Terrane,

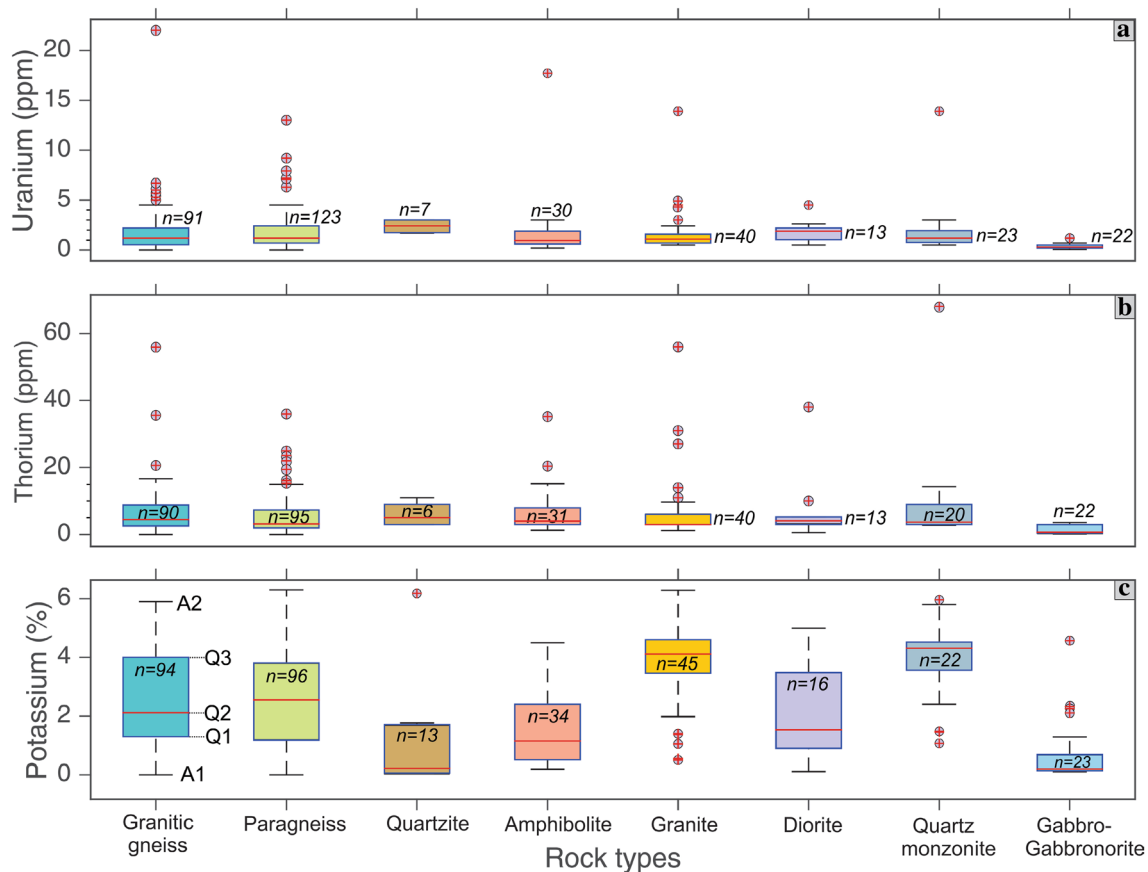


**Fig. 3** Boxplot of the concentration of radiogenic elements **a** uranium (ppm), **b** thorium (ppm) and **c** potassium (%) for different rock types sampled from outcrops in the Grenville Province including the Portneuf-Mauricie (PM) Domain, Morin Terrane (MT) and Parc des Laurentides Domain (PDL). *n* the number of samples,

*Q1* the first quartile value, *Q2* median value, *Q3* the third quartile value,  $A1 = Q1 - 1.5 \times (Q3 - Q1)$ , is the smallest non-outlier value;  $A2 = Q3 + 1.5 \times (Q3 - Q1)$ , is the largest non-outlier value. The circular symbols represent extreme outlier values

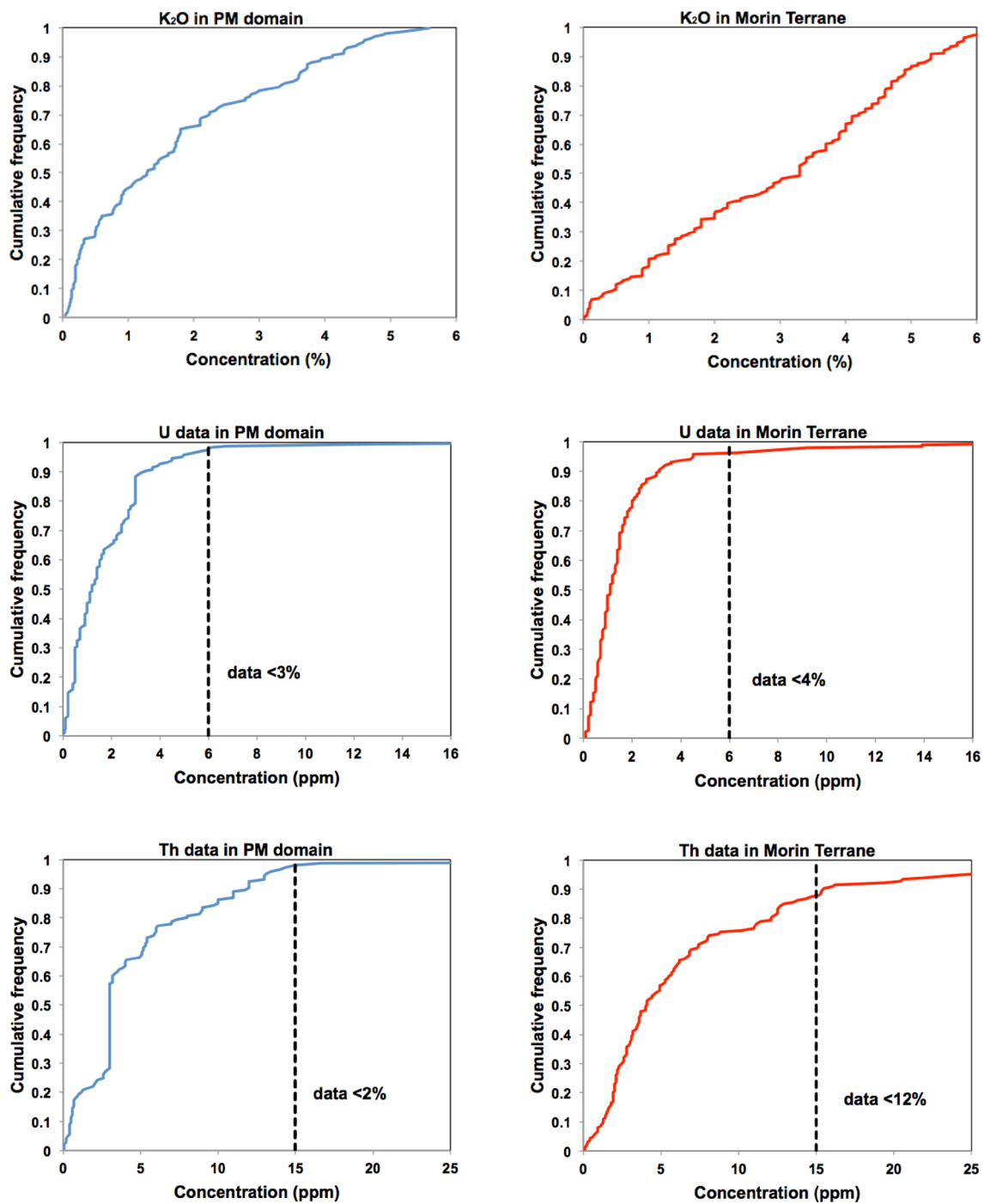


**Fig. 4** Cumulative distribution curves for  $K_2O$ , uranium (U) and thorium (Th) concentrations in the Portneuf-Mauricie domain and the Morin Terrane

respectively, have a uranium concentration of more than 6 ppm. As regards to thorium concentration, less than 2 and 12% of samples from the Portneuf-Mauricie domain and the Morin Terrane, respectively, have their concentrations higher than 15 ppm. This result demonstrates that radiogenic elements concentration for most samples in

the research region is very low. Besides, the Portneuf-Mauricie domain is less radiogenic compared with the Morin Terrane.

### Kriging estimation of uranium concentration

Results of the experimental semi-variance study and a spherical model fit to raw data for uranium concentration

in the study area (of size 35 km × 80 km) are presented in Fig. 5. It can be observed that the omni-directional isotropic semi-variogram is identical to a spherical structural

**Fig. 5** Omni-directional variogram for the concentration of uranium in the study area and the best fitting spherical model

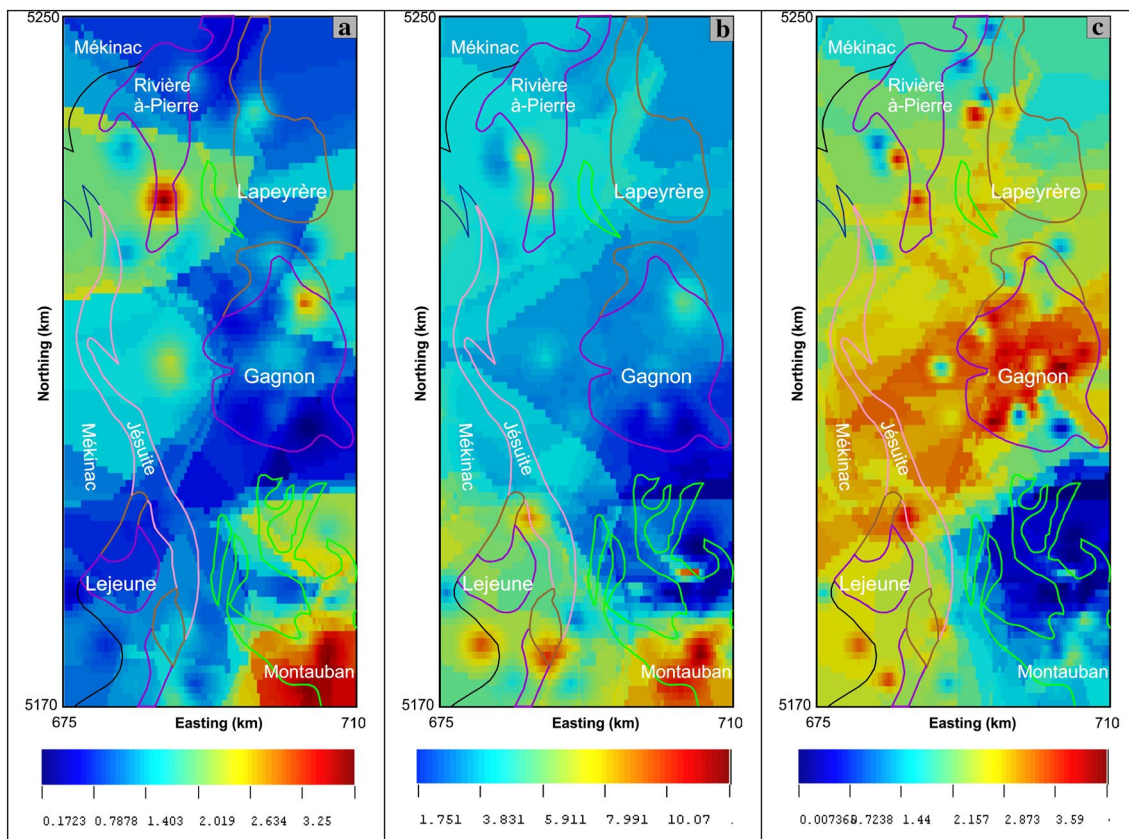
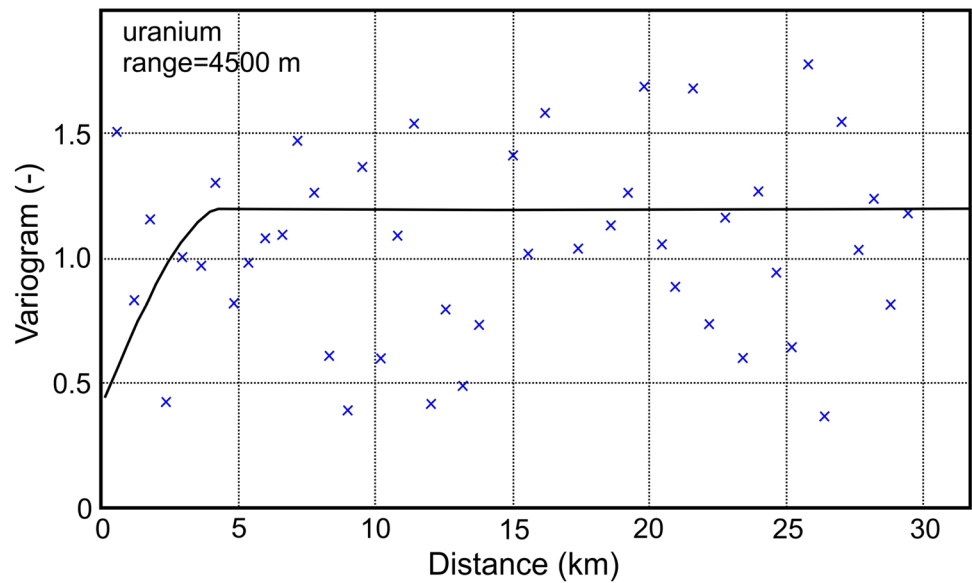


**Fig. 6** Spatial distribution of concentration of **a** uranium (ppm), **b** thorium (ppm) and **c** potassium (%) in the study area obtained through applying the ordinary kriging method (note: the sampling locations presented by rectangles and the main geological boundaries by contours)



curve type, however, with a nugget effect of 0.4, and attains a sill of 0.8 (i.e., 1.2–0.4) at a range of 4500 m.

Using the spherical semi-variogram in Fig. 5 and a search ellipsoid range of 20 km for ordinary kriging estimation, Fig. 6a–c shows the variations in the concentration of radiogenic elements uranium, thorium and potassium, respectively, in the study area. When these results of Figs. 2 and 6 are compared, it can be seen that the ordinary kriging methods describe local estimates better. However, the overall distribution of the concentration is poorly illustrated because of sample limitation.

### Spatial distribution of uranium, thorium and potassium based on SGS

Based on SGS modelling method and the omni-directional semi-variograms shown in Fig. 5, the spatial distribution of uranium (under 100 realizations) is generated in the study area of  $35 \times 80 \text{ km}^2$ , for a cell size of  $175 \text{ m} \times 400 \text{ m}$  using the geostatistics software—SGeMS.

Compared with the distribution of the uranium concentration using ordinary kriging interpolation method (Fig. 6) and the omni-directional variogram with a range

of 3400 m for raw data after normal score transformation (as in Fig. 7a), SGS gives much more details for calculating the concentration of uranium by avoiding the smoothing effect (see Fig. 8a). In ordinary kriging method, the overall distribution of the uranium concentration cannot be described because of the limitation of the data set in the concentration of uranium. In contrast, the sequential Gaussian simulation method can better describe the structure of the database (e.g., uranium concentration, in Fig. 8a) using the probability distribution function. Table 1 presents the range of variations for measured uranium data, E-type from the SGS and the results from the ordinary kriging method. Results obtained from the E-type tallies well with those derived from the ordinary kriging method.

In addition to the uranium concentration, the distribution of the thorium (Fig. 8b) and potassium (Fig. 8c) using SGS simulation method are also shown by applying the results of omni-directional variograms with the range of 7200 m and 6000 m, respectively (Fig. 7b, c). Minor differences occur in the E-type results derived from the two different realizations 30 and 100, demonstrating that the E-type based on the SGS simulation can still be further applied.

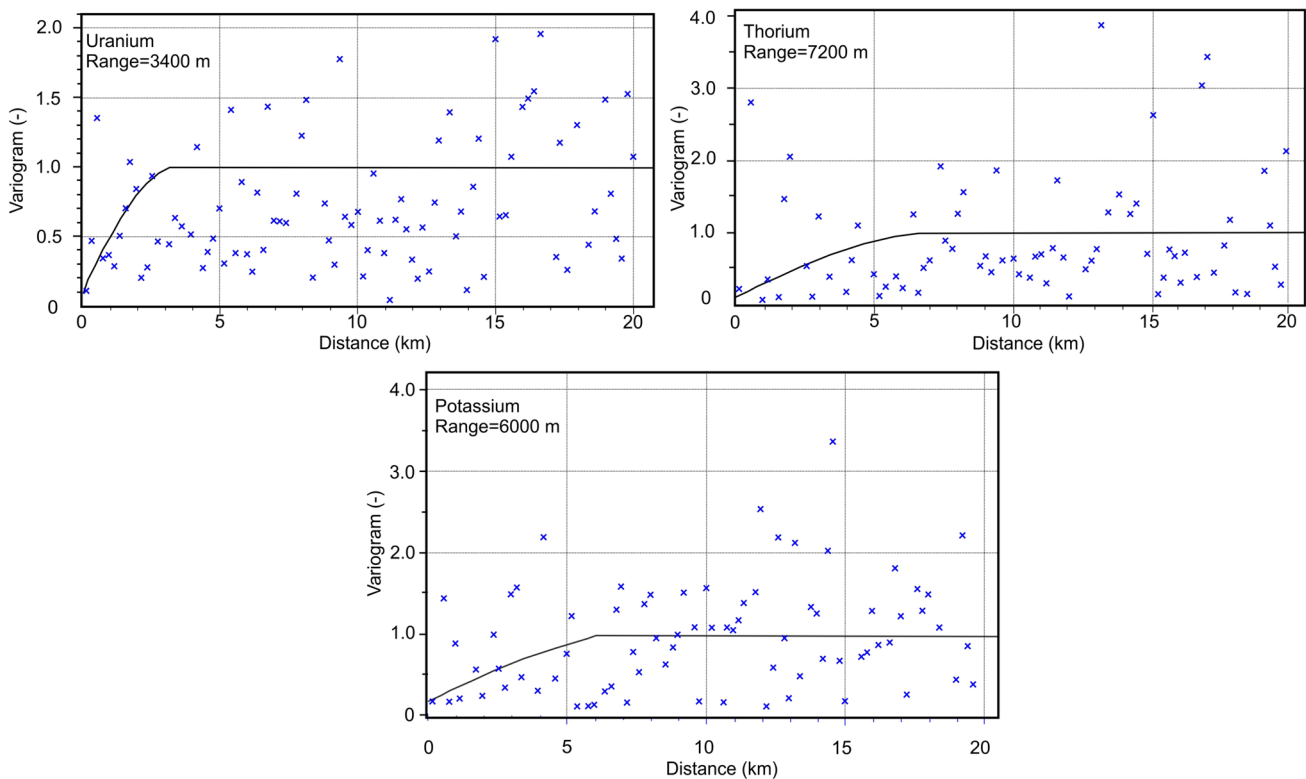


**Fig. 7** Omni-directional variograms for the concentration of uranium, thorium and potassium after the normal score transformation in the study area used for the sgs simulation

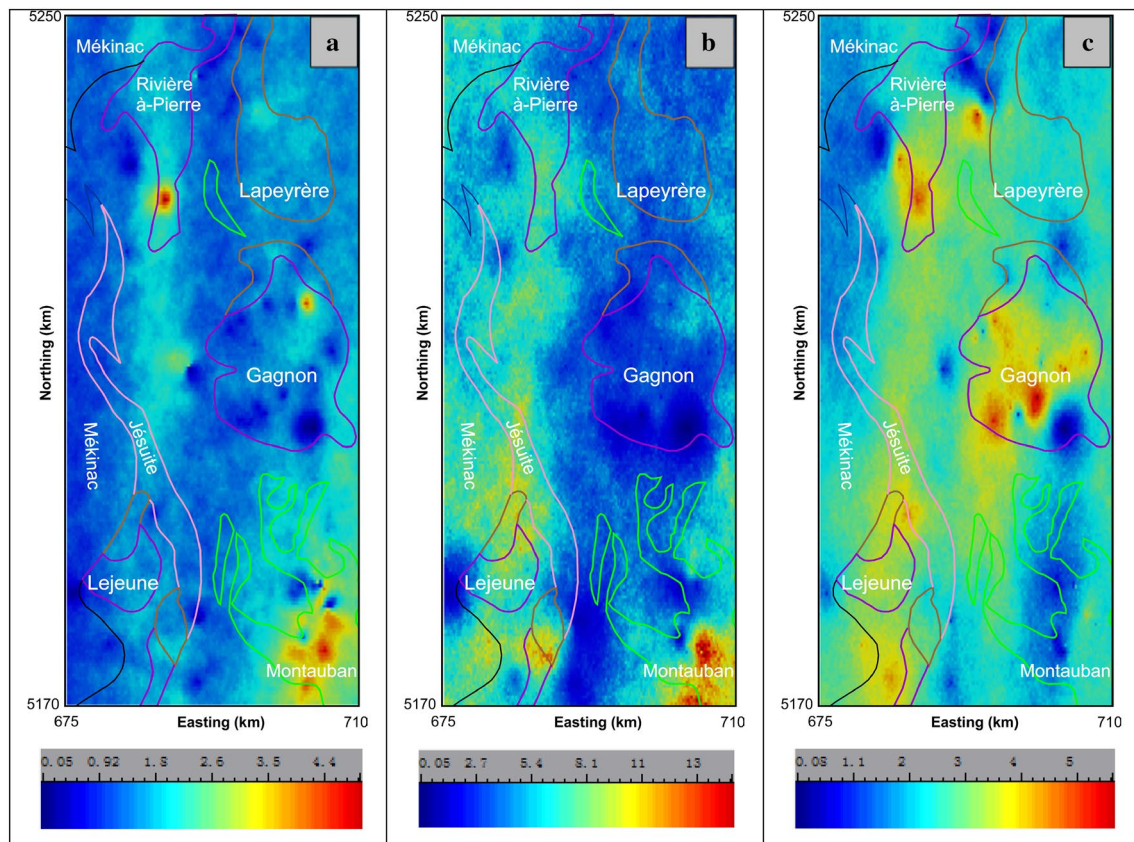


**Fig. 8** Concentration of uranium (a), thorium (b) and potassium (c) using conditional SGS simulation based on 100 realizations applying the omni-directional variograms in Fig. 7

**Table 1** Basic statistics of uranium output data for different realizations, a comparison for raw data, E-type and kriged values

	Range (ppm)	Min (ppm)	Max (ppm)	Mean (ppm)	Variance (ppm)
Raw data	4.850	0.050	4.900	1.460	1.184
E-type	3.360	0.142	3.502	1.383	0.344
Kriged	3.209	0.208	3.417	1.319	0.348

### Spatial distribution of radiogenic heat production based on SGS

In the study area, not all data points that were measured the concentration of the radiogenic elements have the density values. Data points without density values were assigned values based on a data set from the neighboring regions according to the similar rock types. There is a large range of density for a specific rock over a large region, as shown in Fig. 1b, e.g., the density of gabbro ranges from 2600 to 3530 kg/m<sup>3</sup>, with a mean of 2995 kg/m<sup>3</sup>, granite ranges from 2620 to 2760 kg/m<sup>3</sup>, with a mean of 2670 kg/m<sup>3</sup>, granitic gneiss ranges from 2530 to 3160 kg/m<sup>3</sup>, with a mean of 2650 kg/m<sup>3</sup>, granodiorite ranges from 2730 to 2970 kg/m<sup>3</sup>, with a mean of 2840 kg/m<sup>3</sup> etc. Therefore, radiogenic heat production can only be

calculated using the empirical function Eq. 9 when the concentration of uranium, thorium, potassium and their density values are known. Accordingly, three types of radiogenic heat production can be calculated based on the range of the rock density values (i.e., minimum, average and maximum). Afterwards, the spatial distribution of the heat production can be simulated by applying the SGS method (Fig. 9). Result shows that using average densities, the heat production is in the range of 0.01–3.4 μW/m<sup>3</sup>. The difference between calculated radiogenic heat production using the minimum and maximum density values can reach to an extent of 30%, see Fig. 8a, c for comparison.

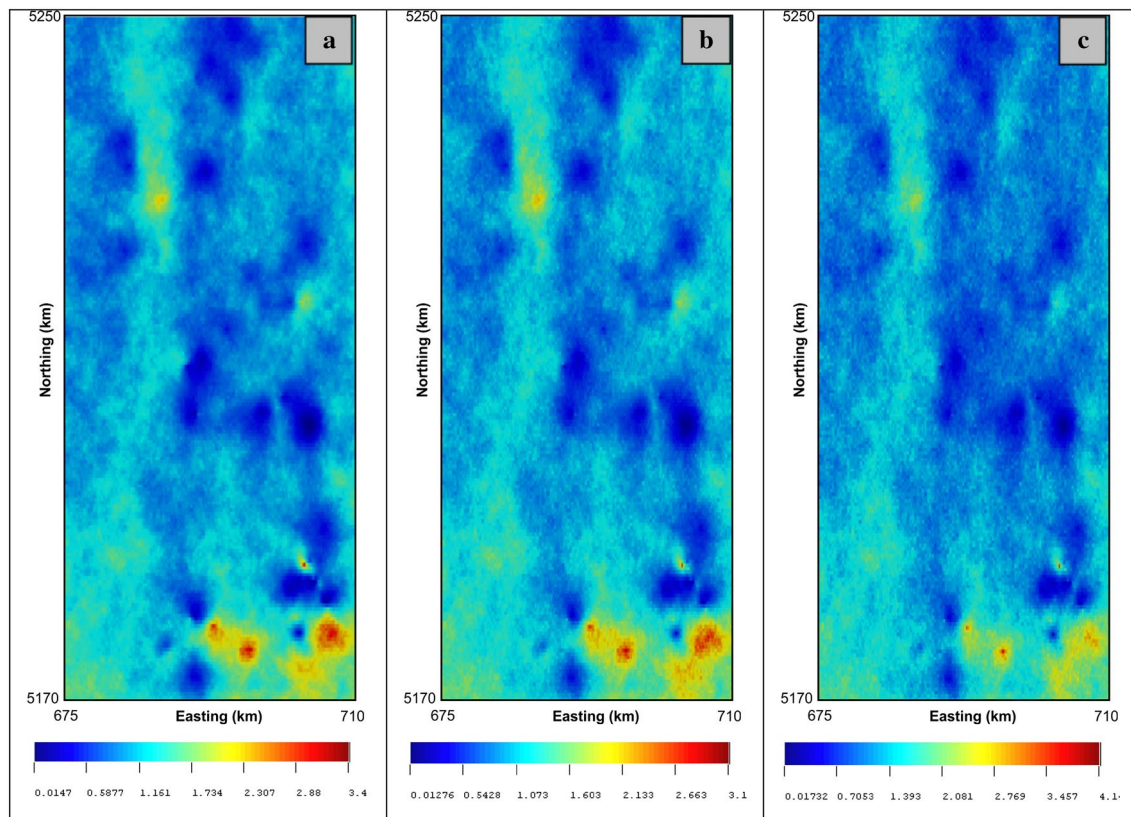


**Fig. 9** Spatial distribution of the radiogenic heat production (unit:  $\mu\text{W}/\text{m}^3$ ) using the average (a), minimum (b) and maximum (c) density values for specific rocks at the sample points through applying the conditional SGS with 100 realizations

## Conclusions

Knowledge of the radiogenic characteristics of the crystalline basement of the western St. Lawrence Lowlands Basin is essential to evaluate the potential of geothermal resources at depth. Since data are typically sparse and expensive to acquire, the radiogenic characteristics of the outcrops in the neighboring Grenville Province may provide a good reference in understanding the heterogeneity of the basement buried by sedimentary rocks in the western St. Lawrence Lowlands Basin. Both the ordinary kriging and the sequential Gaussian simulation methods were applied to analyse the spatial distribution of radiogenic element concentration in a selected region of size  $35 \text{ km} \times 80 \text{ km}$  to calculate the spatial distribution of radiogenic heat production.

Some main conclusions can be drawn as follows: (1) for most rocks from the study region that may represent the granitic basement of the western St. Lawrence Lowlands Basin, the concentration of uranium, thorium and potassium is in the range of 1–2 ppm, 3–10 ppm and 1–4%, respectively; (2) a strong anisotropy exists in the distribution of the radiogenic elements concentration data; (3) compared with the ordinary kriging method, which is better in describing the estimates at a local scale, SGS gives much more details

for calculating the concentration of radiogenic elements in the overall region when data are very sparse; (4) the spatial distribution of radiogenic heat production in the study area is highly dependent on the value of rock density, and concentrations of the radiogenic elements uranium, thorium and potassium; and (5) using the sequential Gaussian simulation method the difference between the minimum and the maximum radiogenic heat production values is 30%, considering the differences in radiogenic element concentration values and different rock density values.

**Acknowledgements** The authors would also like to acknowledge the support received from the CAS Pioneer Hundred Talents Program in China (Y826031C01). Special thanks to Bernard Giroux and Erwan Gloaguen at INRS-ETE for their invaluable help with the technical support in using the SGeMS software. Thanks to Aurelie Gicquel for providing some radiogenic elements data from the research region.

## References

- Caers J (2005) Petroleum geostatistics. SPE, Kuala Lumpur
- Davidson A (1984) Identification of ductile shear zones in the south-western Grenville Province of the Canadian Shield. In: Kroner A, Greiling R (eds) Precambrian tectonics illustrated. Schweitzerbart'sche Verlagsbuchhandlung, Stuttgart, pp 263–279

- Delbari M, Afrasiab P, Loiskandl W (2009) Using sequential Gaussian simulation to assess the field-scale spatial uncertainty of soil water content. *Catena* 79:163–169
- Deutsch C, Journel AG (1998) *GSLIB: geostatistical software library and users's guide*, 2nd edn. Oxford University Press, New York, p 340
- Doyen PM (2007) Seismic reservoir characterization: an earth modelling perspective. EAGE, Houten
- Dubrule O (1989) A review of stochastic models for petroleum reservoirs. In: Armstrong M (ed) *Quantitative geology and geostatistics*. Springer Netherlands, Dordrecht, pp 493–506
- Dufréchéou G, Harris LB, Corriveau L (2014) Tectonic reactivation of transverse basement structures in the Grenville orogeny of SW Quebec, Canada: insights from gravity and aeromagnetic data. *Precamb Res* 241:61–84
- Fichter LS, Richard JD (1993) Evidence for the progressive closure of the Proto-Atlantic ocean in the valley and ridge province of Northern Virginia and Eastern West Virginia. In: field trip guide, National Association of Geology Teachers—Eastern Section Meeting, James Madison University
- Fuchs S, Balling N (2016) Improving the temperature predictions of subsurface thermal models by using high-quality input data. Part 1: uncertainty analysis of the thermal-conductivity parameterization. *Geothermics* 64:42–54
- Goovaerts P (1997a) *Geostatistics for natural resources evaluation*. Oxford University Press, New York, p 483
- Goovaerts P (1997b) Kriging vs stochastic simulation for risk analysis in soil contamination. In: Soares A, Gomez-Hernandez J, Froidevaux R (eds) *geoENV I-Geostatistics for environmental applications, series quantitative geology and geostatistics*, vol 9, pp 247–258
- Hatcher RD Jr, Bream BR, Miller CF, Eckert JO Jr, Fullagar PD, Carrigan CW (2004) Paleozoic structure of internal basement massifs, southern Appalachian Blue Ridge, incorporating new geochronologic, Nd and Sr isotopic, and geochemical data. In: Tollo RP, Corriveau L, McLelland J, Bartholomew MJ (eds) *Proterozoic tectonic evolution of the Grenville orogen in North America*, vol 197. Geological Society of America Memoir, Boulder, pp 525–547
- Krige DG (1951) A statistical approach to some mine valuations problems at the Witwatersrand. *J Chem Metall Min Soc S Afr* 52:119–139
- Lavoie D, Pinet N, Castonguay S, Dietrich J, Giles P, Fowler M, Thériault R, Laliberté JY P, St, Hinds S, Hicks L, Klassen H (2009) Hydrocarbon systems in the Paleozoic basins of eastern Canada—Presentations at the Calgary 2007 workshop, Geological Survey of Canada Open File 5980, pp 9–79
- Li J, Heap AD (2008) A review of spatial interpolation methods for environmental scientists. *Geoscience Australia. Record* 2008/23, p 137
- Li J, Heap AD (2014) Spatial interpolation methods applied in the environmental sciences: a review. *Environ Model Softw* 53:173–189
- Mareschal JC, Jaupart C (2004) Variations of surface heat flow and lithospheric thermal structure beneath the North American craton. *Earth Planet Sci Lett* 223:65–77
- Matheron G (1963) Principles of geostatistics. *Eco Geol* 58:1246–1266
- McLelland JM, Selleck BW, Bickford ME (2010) Review of the Proterozoic evolution of the Grenville Province, its Adirondack outlier, and the Mesoproterozoic inliers of the Appalachians. In: Tollo RP, Bartholomew MJ, Hibbard JP, Karabinos PM (eds) *From Rodinia to Pangea: the lithotectonic record of the Appalachian Region*, vol 206. Geological Society of America Memoir, Boulder, pp 1–29
- Meixner AJ, Kirkby AL, Lescinsky DT, Horspool N (2012) The Cooper Basin 3D map version 2: thermal modelling and temperature uncertainty. *Record* 2012/060. Geoscience Australia, Canberra, pp 1–52
- Nadeau L, Brouillette P (1994) Carte structurale de la région de La Tuque (SNRC 31P), Province de Grenville, Québec. Commission Géologique du Canada, dossier public 2938, 1: 250000
- Nadeau L, Brouillette P (1995) Carte structurale de la région de Shawinigan (SNRC 31I), Province de Grenville, Québec. Commission Géologique du Canada, dossier public 3012, 1: 250000
- Nshagali BG, Njandjock Nouck P, Meli'i JL, Aretouyap Z, Manguelle-Dicoum E (2015) High iron concentration and pH change detected using statistics and geostatistics in crystalline basement equatorial region. *Environ Earth Sci* 73:7135–7145
- Olea RA (1999) *Geostatistics for engineers and earth scientists*. Kluwer Academic Publishers, Dordrecht, p 303
- Pinti DL, Béland-Otis C, Tremblay A, Castro MC, Hall CM, Marcil J-S, Lavoie J-Y, Lapointe R (2011) Fossil brines preserved in the St-Lawrence Lowlands, Québec, Canada as revealed by their chemistry and noble gas isotopes. *Geochim Cosmochim Acta* 75:4228–4243
- Remy N, Boucher A, Wu J (2009) *Applied geostatistics with SGEMS: a user's guide*. Cambridge University Press, Cambridge
- Rivers T (1983) The northern margin of the Grenville Province in western Labrador—atomy of an ancient orogenic front. *Precamb Res* 22:41–73
- Rivers T (2015) Tectonic setting and evolution of the Grenville orogeny: an assessment of progress over the last 40 years. *Geosci Can* 42:77–124
- Rybach L (1976) Radioactive heat production in rocks and its relation to other petrophysical parameters. *Pure Appl Geophys* 114:309–318
- Rybach L (1988) Determination of heat production rate. In: Hanel R, Rybach L, Stegena L (eds) *Handbook of terrestrial heat flow determination*. Kluwer Academic Publishers, Dordrecht, pp 125–142
- Sappin A-A (2012) *Pétrologie et métallogénie d'indices de Ni-Cu-éléments du Groupe du Platine du Domaine de Portneuf-Mauricie, Québec (Canada)*, Thèse de doctorat at Université Laval, p 70
- Shumaker RC, Wilson TH (1996) Basement structure of the Appalachian foreland in West Virginia: its style and effect on sedimentation. In: Van der Pluijm BA, Catacosinos PA (eds), *Basement and basins of Eastern North America*. Geological Society of America, Boulder, pp 139–155
- SIGEOM (2018) <http://sigeom.mines.gouv.qc.ca>
- Soltani F, Afzal P, Asghari O (2013) Sequential Gaussian simulation in the Sungun Cu porphyry deposit and comparing the stationary reproduction with ordinary kriging. *Univ J Geosci* 1(2):106–113
- Song HB, Zhang ML, Sheng JC, Luo YL (2013) Stochastic simulation of fluid flow in porous media by the complex variable expression method. *J Hydrodyn* 25(2):215–225
- Tester J, Anderson BJ, Blackwell DD, DiPippo R et al (2006) The future of geothermal energy—impact of enhanced geothermal systems (EGS) on the United States in the 21st century. Massachusetts Institute of Technology, Cambridge
- Tremblay A, Long B, Massé M (2003) Supracrustal faults of the St. Lawrence rift system, Québec: kinematics and geometry as revealed by field mapping and marine seismic reflection data. *Tectonophysics* 369:231–252
- Vidal A, Archer R (2015) Geostatistical simulations of geothermal reservoirs: two-and multiple-point statistic models. In: *Proceedings World geothermal congress 2015*, Melbourne, Australia, 19–25 April 2015
- Yamamoto JK (2000) An alternative measure of the reliability of ordinary kriging estimates. *Math Geol* 32(4):489–509
- Yang FG, Cao SY, Liu XN, Yang KJ (2008) Design of groundwater level monitoring network with ordinary kriging. *J Hydrodyn* 20(3):339–346
- Zhao YF, Sun ZY, Chen J (2010) Analysis and comparison in arithmetic for kriging interpolation and sequential Gaussian conditional simulation. *J Geo Inform Sci* 12(6):767–776